The Th17–ELR$^+$ CXC chemokine pathway is essential for the development of central nervous system autoimmune disease

Thaddeus Carlson,[1] Mark Kroenke,[1] Praveen Rao,[1] Thomas E. Lane,[3] and Benjamin Segal[1,2]

[1]Department of Microbiology and Immunology and [2]Department of Neurology, University of Rochester School of Medicine and Dentistry, Rochester, NY 14642
[3]Department of Molecular Biology and Biochemistry and Center for Immunology, University of California, Irvine, Irvine, CA 92697

The ELR$^+$ CXC chemokines CXCL1 and CXCL2 are up-regulated in the central nervous system (CNS) during multiple sclerosis (MS) and its animal model, experimental autoimmune encephalomyelitis (EAE). However, their functional significance and the pathways regulating their expression are largely unknown. We show that transfer of encephalitogenic CD4$^+$ Th17 cells is sufficient to induce CXCL1 and CXCL2 transcription in the spinal cords of naive, syngeneic recipients. Blockade or genetic silencing of CXCR2, a major receptor for these chemokines in mice, abrogates blood–brain barrier (BBB) breakdown, CNS infiltration by leukocytes, and the development of clinical deficits during the presentation as well as relapses of EAE. Depletion of circulating polymorphonuclear leukocytes (PMN) had a similar therapeutic effect. Furthermore, injection of CXCR2$^+$ PMN into CXCR2$^{-/-}$ mice was sufficient to restore susceptibility to EAE. Our findings reveal that a Th17–ELR$^+$ CXC chemokine pathway is critical for granulocyte mobilization, BBB compromise, and the clinical manifestation of autoimmune demyelination in myelin peptide–sensitized mice, and suggest new therapeutic targets for diseases such as MS.

CORRESPONDENCE
Benjamin M Segal:
bmsegal@umich.edu

Abbreviations used: BBB, blood–brain barrier; BMMac, enriched bone marrow macrophages; CNS, central nervous system; EAE, experimental autoimmune encephalomyelitis; MS, multiple sclerosis; NP, influenza nucleoprotein; NRS, normal rabbit serum; PGRP, peptidoglycan recognition protein; PLP, proteolipid protein.

Experimental autoimmune encephalomyelitis (EAE) is a CD4$^+$ T cell–driven autoimmune disease that shares clinical and histological similarities with multiple sclerosis (MS). In EAE, CD4$^+$ T cells specific for antigens expressed in central nervous system (CNS) myelin initiate a localized inflammatory process that results in demyelination, axonal transection, and clinical deficits. Active EAE and MS lesions are characterized by perivascular infiltrates predominantly composed of myeloid cells (macrophages, dendritic cells, and activated microglia) and lymphocytes (1, 2). Consequently, a large body of research has focused on the role of ML chemokines (particularly CCL1, CCL2, CCL3, and CCL5) and ELR$^-$ CXC chemokines (such as CXCL10) in the recruitment of circulating lymphocytes and monocytes to the CNS during EAE and MS (3, 4).

ELR$^+$ CXC chemokines, such as CXCL1 and CXCL2 in mice and CXCL8 in humans, are also up-regulated in EAE lesions (where they localize to astrocytes and, to some extent, microglia) and in the peripheral blood mononuclear cells and cerebrospinal fluid of MS patients (5–10). These chemokines are potent attractants for PMN. Hence, in mouse models of pulmonary aspergillosis (toxoplasmosis and staphylococcal cerebritis), expression of CXCR2, a major receptor for ELR$^+$ CXC chemokines in mice, is critical for the accumulation of PMN at sites of inflammation and, consequently, eradication of microbial pathogens (11–13). Furthermore, blockade of CXCR2 prevents inflammation and tissue destruction in experimental models of arthritis and CD4$^+$ T cell–mediated hypersensitivity reactions in the lungs, both of which entail PMN-rich inflammatory infiltrates in the target organ (14, 15). In addition, under certain conditions ELR$^+$ CXC chemokines mediate monocyte arrest. For example, they play a critical role in monocyte infiltration in atherosclerotic plaques (16).

Relatively little is known about the biological significance or cellular target of ELR$^+$ CXC chemokines in the development and/or

The online version of this article contains supplemental material.

maintenance of autoimmune demyelinating disease, in which infiltrates are dominated by lymphocytes and monocytes. Although PMN have been detected entering the CNS during the preclinical phase of EAE (17), their relative paucity in mature EAE and MS lesions has led some investigators to question their importance (8). With regard to more populous myeloid subsets in EAE and MS lesions, activated macrophages are recruited to the CNS by a CCL2-dependent pathway across several EAE models (18). Perhaps because of such observations, the role of ELR$^+$ CXC chemokines in the pathophysiology of autoimmune demyelination has not been previously investigated in depth. However, a growing body of data indicates that they merit attention. For example, IL-17, a potent inducer of ELR$^+$ CXC chemokines, was recently implicated in the pathogenesis of both EAE and MS (19–21). In addition, McColl et al. found that in vivo depletion of PMN prevents acute EAE induced either by active immunization or adoptive transfer (22). Interestingly, PMN comprise a significant percentage of CNS-infiltrating leukocytes in an atypical and severe form of EAE manifested by IFN-γ and IFN-γ receptor knockout mice, as well as in aggressive forms of human inflammatory demyelinating disease, such as Marburg's variant of MS and hemorrhagic leukoencephalitis, suggesting that these cells might directly promote CNS inflammation and/or white matter injury (9, 23, 24). Collectively, these findings led us to comprehensively examine for the first time the role of CXCR2 and ELR$^+$ CXC chemokines in conventional EAE models, to investigate the relationship between TH17 cell infiltration and ELR$^+$ CXC chemokine expression in the CNS, and to specifically address whether PMN activation/recruitment via ELR$^+$ CXC chemokine pathways is necessary for the development of relapses after clinical onset.

RESULTS

CNS expression of ELR$^+$ CXC chemokines and CXCR2 mirrors clinical disease activity during relapsing-remitting EAE

To determine the pattern of ELR$^+$ CXC chemokine expression throughout the course of relapsing-remitting disease, we immunized SJL mice with an immunodominant epitope of proteolipid protein ($PLP_{139-151}$) in CFA and measured CNS expression of CXCL1 and CXCL2 mRNA in samples grouped according to clinical stage. In agreement with earlier reports (5–8), we found that CNS CXCL1 and CXCL2 were up-regulated from baseline levels (as measured in spinal cords from naive mice) at the peak of clinical EAE (Fig. 1 A). Expression of both chemokines fell to baseline during the subsequent remission and rebounded during relapse. Peptidoglycan recognition protein (PGRP), a PMN-specific marker (25), and CXCR2, an ELR$^+$ CXC chemokine receptor expressed predominantly by PMN, exhibited similar kinetics. The same was true of the proinflammatory T cell effector cytokines IL-17 and IFN-γ and the ML chemokine CCL2. In contrast, CCL19 transcripts were elevated during the initial episode but progressively fell with each successive stage, whereas CCL3 and CCL5 transcripts were stable at a heightened level throughout the course. IL-10 was not elevated to a statistically significant extent at any stage. Expression of every chemokine and cytokine in our panel remained at baseline levels across multiple time points in spinal cords of mice immunized with an immunodominant epitope of influenza nucleoprotein ($NP_{260-283}$).

As mentioned earlier, PMN have been detected crossing the blood–brain barrier (BBB) during the preclinical stage of EAE, when inflammatory infiltrates are beginning to form but before the manifestation of neurological deficits (17). Therefore, we measured CNS CXCL1 and CXCL2 on a daily basis starting on day 3 after immunization with $PLP_{139-151}$. Transcripts encoding CXCL1 and CXCL2, as well as CXCR2 and PGRP, were detectable above baseline levels as early as 4 d before the expected day of clinical onset and increased progressively thereafter (Fig. 1 B). CD4, IL-17, and IFN-γ mRNA followed a similar pattern. In contrast, transcripts encoding CCL2, CCL3, CCL5, and CCL19 rose above baseline at later time points than the ELR$^+$ CXC chemokines, suggesting that PMN may be actively recruited to the spinal cord before most other inflammatory cells. IL-10 was transcribed at a low level that did not change during the course of disease.

Transfer of purified myelin-reactive CD4$^+$ Th17 cells is sufficient to induce CXCL1 and CXCL2 expression in the CNS

Th17 cells have recently been implicated in the pathogenesis of EAE and MS, as well as other organ-specific autoimmune diseases (19–21). IL-17 stimulates ELR$^+$ CXC chemokine production in multiple cell types. Therefore we questioned whether transfer of myelin-specific CD4 Th17 cells would be sufficient to induce CXCL1 and CXCL2 transcription in the spinal cords of naive, syngeneic hosts. Purified CD4$^+$ T cells, from donor SJL mice primed with $PLP_{139-151}$ in IFA, were challenged with antigen for 96 h in the presence of recombinant IL-23, IL-12, or a neutralizing antibody against the IL-12/IL-23 p40 chain before injection into previously unmanipulated syngeneic hosts. PLP-reactive T cells proliferated in a similar fashion (Fig. 2 A, right) and expanded to a similar extent (based on yields of viable lymphoblasts; not depicted) under each set of culture conditions in vitro. As expected, IL-23–stimulated cells secreted large quantities of IL-17, whereas IL-12–stimulated cells secreted large quantities of IFN-γ during antigenic challenge in vitro (Fig. 2 A, left). Cells cultured with anti-p40 produced neither of those cytokines to detectable levels. IL-23–stimulated cells preferentially induced expression of IL-17 mRNA in spinal cords of adoptive transfer recipients (Fig. 2 B). In contrast, IL-12–stimulated cells induced CNS up-regulation of IFN-γ but not IL-17.

Spinal cords from mice injected with IL-23–driven Th17 cells expressed dramatically elevated levels of CXCL1 and CXCL2, as well as PGRP (a neutrophil-specific marker) and G-CSF, compared with cords from naive mice (Fig. 2 B and not depicted). In contrast, those molecules remained at background levels in spinal cords from mice injected with PLP-reactive CD4$^+$ T cells that had been reactivated in the

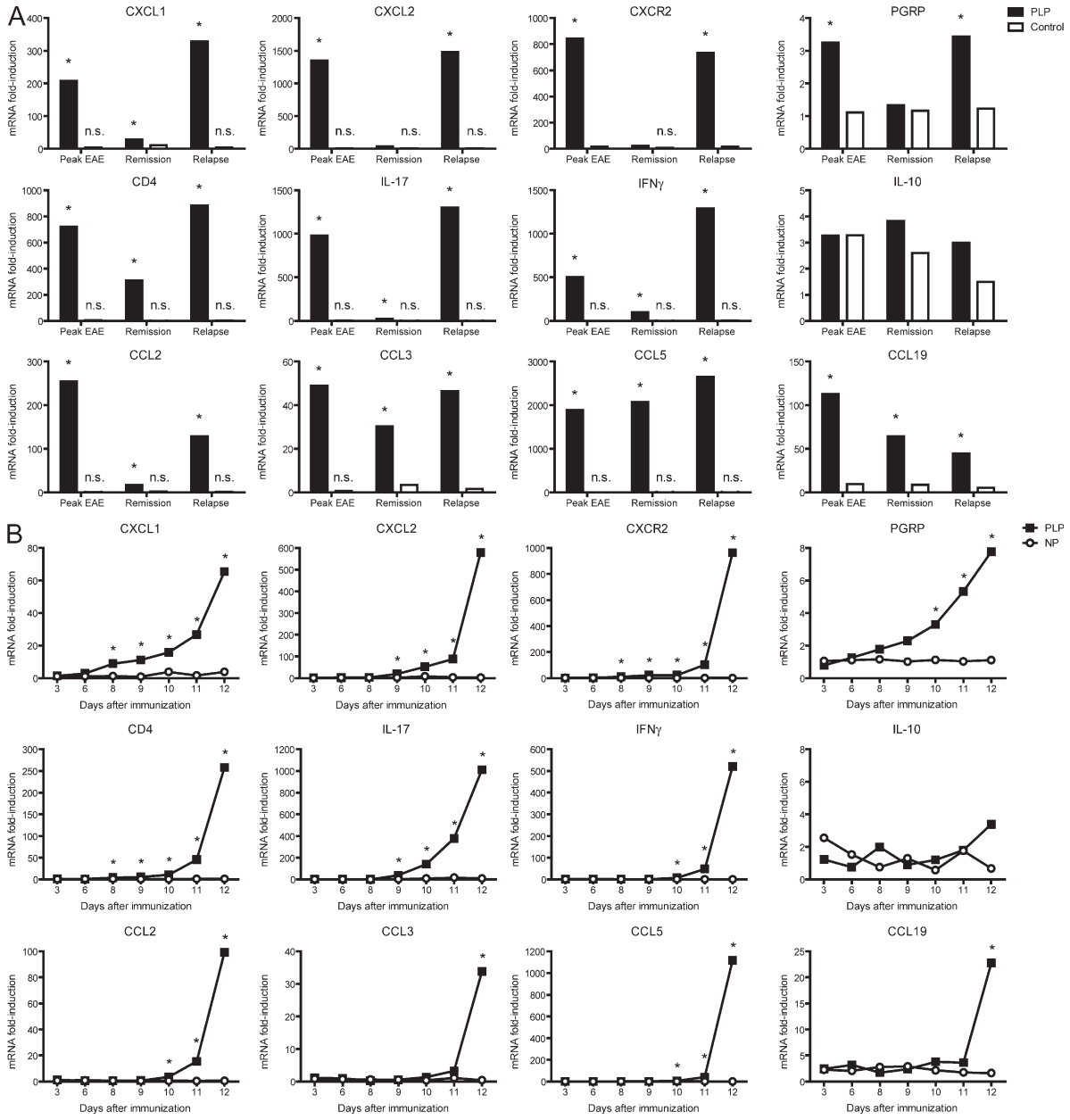

Figure 1. ELR+ CXC chemokines are up-regulated in the CNS during preclinical and active stages of EAE. (A) SJL mice were immunized with $PLP_{139-151}$ or $NP_{260-283}$ (control) in CFA. Spinal cord RNA was isolated from $PLP_{139-151}$–primed mice during distinct stages of EAE, or from $NP_{260-283}$–primed mice at analogous time points after immunization, for real-time RT-PCR analysis. Data represent fold induction compared with naive spinal cords ($n = 4$ mice per group). (B) RNA was extracted from spinal cords between days 8 and 12 after immunization with $PLP_{139-151}$ or $NP_{260-283}$ for analysis by real-time RT-PCR ($n = 5$ mice per group). *, $P < 0.05$ for PLP-immunized mice compared with NP-immunized mice. n.s., not significantly different from naive spinal cords.

presence of anti–IL-12 p40. By comparison to the Th17 effectors, IL-12–driven Th1 cells were relatively inefficient at inducing ELR^+ CXC chemokines in the CNS. Of note, PLP-specific donor T cells from each set of cultures survived/expanded to a comparable extent in the peripheral lymphoid organs of host mice, as assessed by lymphoproliferative recall responses on day 14 after transfer (unpublished data). Splenocytes harvested from recipients of IL-23–polarized cells secreted IL-17 and splenocytes from recipients of IL-12–polarized cells secreted IFN-γ in an antigen-specific manner, suggesting that the donor cells maintained their Th phenotypes after adoptive transfer (unpublished data).

CXCR2 blockade abrogates EAE

To assess the physiological significance of ELR^+ CXC chemokine expression in our model, we injected SJL mice with either anti-CXCR2 antiserum or normal rabbit serum (NRS) between days 8 and 14 after immunization with $PLP_{135-151}$ (13).

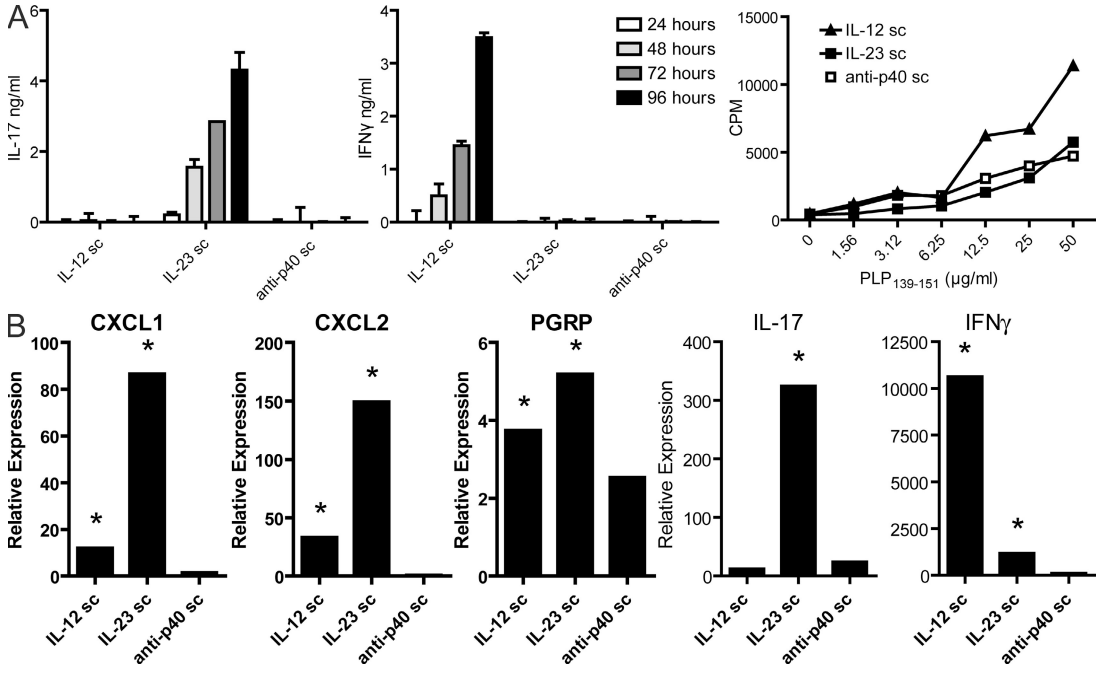

Figure 2. Transfer of myelin-reactive Th17 cells induces CNS expression of CXCL1 and CXCL2. LN cells from donor SJL mice immunized with $PLP_{139-151}$ in IFA were cultured with antigen in the presence of either recombinant IL-23 (for the generation of Th17 cells), IL-12 (for the generation of Th1 cells), or anti–IL-12/23 p40 neutralizing antibody (for the generation of lineage-uncommitted cells). (A, left and middle) Supernatants were collected serially and subjected to ELISA for measurement of IL-17 and IFN-γ levels. (A, right) Some wells were pulsed with tritiated thymidine at 72 h and harvested 12 h later for measurement of radioisotope incorporation. Data represent mean ± SD. (B) Spinal cords were harvested from hosts that had been injected with either Th17, Th1, or uncommitted $PLP_{139-151}$–reactive T cells 10 d earlier (n = 5 mice per group). RNA was extracted for analysis by real-time RT-PCR. The results show mean relative expression of the specified transcripts in cords from host mice to cords from naive mice. A representative experiment of four is shown. *, $P < 0.05$ compared with naive mice.

Anti-CXCR2 treatment significantly reduced mean clinical EAE scores (Fig. 3 A). Mice that were asymptomatic during treatment with anti-CXCR2 developed EAE within 2–3 d of the last injection of antiserum, in agreement with the onset of relapse in the control group. Of greater clinical relevance, administration of anti-CXCR2 during remission completely suppressed subsequent relapse (Fig. 3 B).

Anti-CXCR2 treatment prevented BBB breakdown, the development of inflammatory infiltrates, and up-regulation of proinflammatory cytokines (IL-17, IL-6, and IFN-γ) in the CNS of the protected mice (Fig. 3, C–E). PGRP mRNA did not rise above background levels, indicating that PMN had failed to enter the CNS. In contrast, $CD4^+$ T cells isolated from lymph nodes and spleens of anti-CXCR2–treated mice mounted robust myelin-specific proliferative responses upon in vitro challenge (Fig. 3 F). Hence, our data indicate that CXCR2–PMN–dependent pathways are necessary for the clinical and histopathological manifestation of EAE despite the presence of activated myelin-specific T cells in the peripheral lymphoid organs.

Administration of anti-CXCR2 in vivo had no effect on the percentage or absolute number of bone marrow PMN in multiple experiments; its effect on circulating PMN was more variable. Anti-CXCR2 does not facilitate complement-mediated lysis of neutrophils in vitro (unpublished data). Collectively these data suggest that the therapeutic effect of anti-CXCR2 may be secondary to blockade of PMN mobilization from the bone marrow into the blood stream.

Experiments using $CXCR2^{-/-}$ (26) mice corroborated our findings with the CXCR2-neutralizing antiserum. In repeated experiments, 90–100% of myelin antigen–primed WT mice developed EAE (mean clinical score = 2–3), signifying conspicuous hind-limb paresis (Fig. 3 G). In contrast, none of the $CXCR2^{-/-}$ mice on the same genetic background that were subjected to the same immunization protocol acquired neurological deficits. $CXCR2^{+/-}$ mice exhibited an intermediate phenotype.

PMN are mobilized from the bone marrow and accumulate in the CNS during preclinical and acute stages of EAE

To monitor the migration of PMN during the development of EAE, we tracked $Ly6G^+$, $7/4^+$, MHC class II^- cells in the circulatory and CNS compartments by flow cytometry. PMN began accumulating in the blood during the preclinical phase, and their percentage among circulating leukocytes rose through peak disease (Fig. 4, A and B). Similarly, PMN appeared in the CNS shortly before the expected day of clinical onset, and their absolute numbers increased in proportion to the growing inflammatory infiltrate (Fig. 4, C and D).

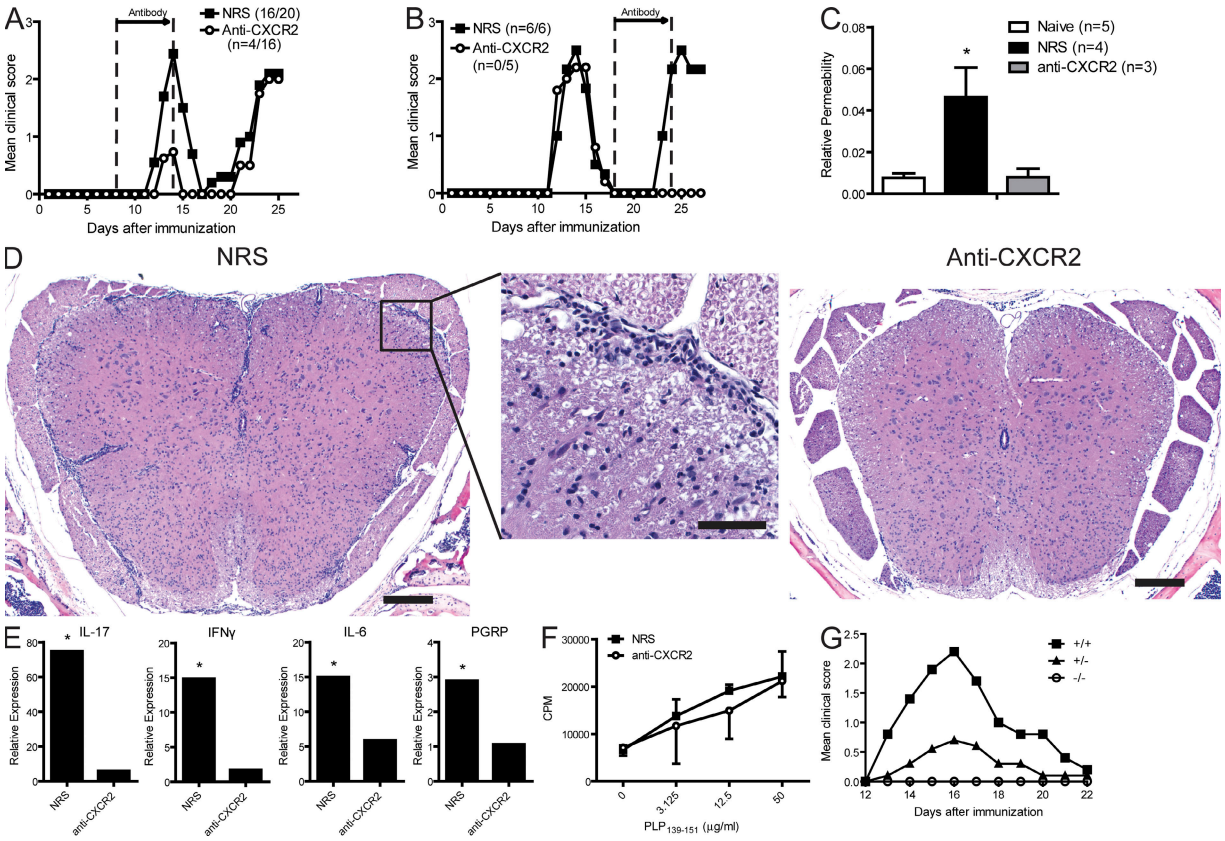

Figure 3. CXCR2 plays a critical role in the presentation and relapse of EAE. Mice immunized with $PLP_{139-151}$ in CFA were treated with anti-CXCR2 antiserum or NRS between days 8 and 14 (A and C–E) or days 18 and 24 (B) after immunization. (A and B) Mice were rated for clinical signs of EAE on a daily basis. (C) BBB integrity was assessed on day 14 after immunization by Evans blue dye extravasation. Relative permeability is calculated as follows: (μg Evans blue/g spinal cord)/(μg Evans blue/g kidney). Data represent mean ± SD. *, $P < 0.05$ compared with naive mice. (D) Spinal cords were fixed on day 14 after immunization. Representative hematoxylin and eosin sections are shown from five mice per group. Bars: (left and right) 200 μm; (middle) 50 μm. (E) Spinal cords were sampled at the time of peak disease in the group injected with NRS and analyzed by real-time RT-PCR. Data represent fold induction relative to naive spinal cords (NRS, $n = 4$; anti-CXCR2, $n = 3$). *, $P < 0.05$ for anti-CXCR2– compared with NRS-treated mice. (F) $CD4^+$ T cells, purified from draining lymph nodes on day 14 after immunization, were stimulated with naive T cell–depleted splenocytes and 25 μg/ml $PLP_{139-151}$ in vitro. Lymphoproliferation was measured by uptake of $[^3H]$thymidine. Data represent mean ± SD. (G) BALB/c $CXCR2^{+/+}$, $CXCR2^{+/-}$, and $CXCR2^{-/-}$ mice were immunized with $PLP_{185-206}$ in CFA to induce EAE. The mean daily clinical score of each group is shown (+/+, $n = 5$; +/−, $n = 8$; −/−, $n = 7$). The experiment was repeated five times with similar results.

Histological analysis confirmed the presence of PMN, based on morphological characteristics, within small perivascular and meningeal infiltrates during the preclinical phase and within mature perivascular and parenchymal infiltrates in mice with neurological deficits (Fig. 4 E).

PMN depletion prevents the initiation and relapse of EAE

To definitively assess the functional relevance of PMN during different stages of relapsing-remitting EAE, we injected PLP-immunized mice with RB6 (an mAb specific for the myeloid marker Gr-1 that has been widely used to deplete PMN in vivo [27]) according to a variety of dosing schedules. We found that RB6 depleted circulating PMN without affecting other leukocyte subsets (Fig. 5 A; and Fig. S1, available at http://www.jem.org/cgi/content/full/jem.20072404/DC1).

Injection of RB6 beginning at preclinical time points prevented BBB breakdown and the development of neurological deficits throughout the duration of treatment (Fig. 5, B and C). However, 2–3 d after the cessation of injections, in agreement with recovery of the circulating PMN pool, we consistently observed an acute increase in cerebrovascular permeability and the onset of hind-limb weakness. Furthermore, initiation of RB6 treatments during remission prevented subsequent cerebrovascular compromise and clinical relapse (Fig. 5, D and E). Histological studies corroborated our clinical findings, demonstrating that RB6 treatment completely inhibited CNS inflammation in PLP-immunized mice (Fig. 5, F and G). Therefore, PMN depletion by RB6 had similar effects to ELR^+ CXC chemokine blockade by anti-CXCR2 in maintaining the integrity of the BBB and preventing the clinical and histological manifestations of EAE.

PMN depletion does not alter peripheral myelin-specific T cell responses

PMN can directly trigger dendritic cell maturation via interactions between Mac-1 and DC-SIGN, thereby boosting

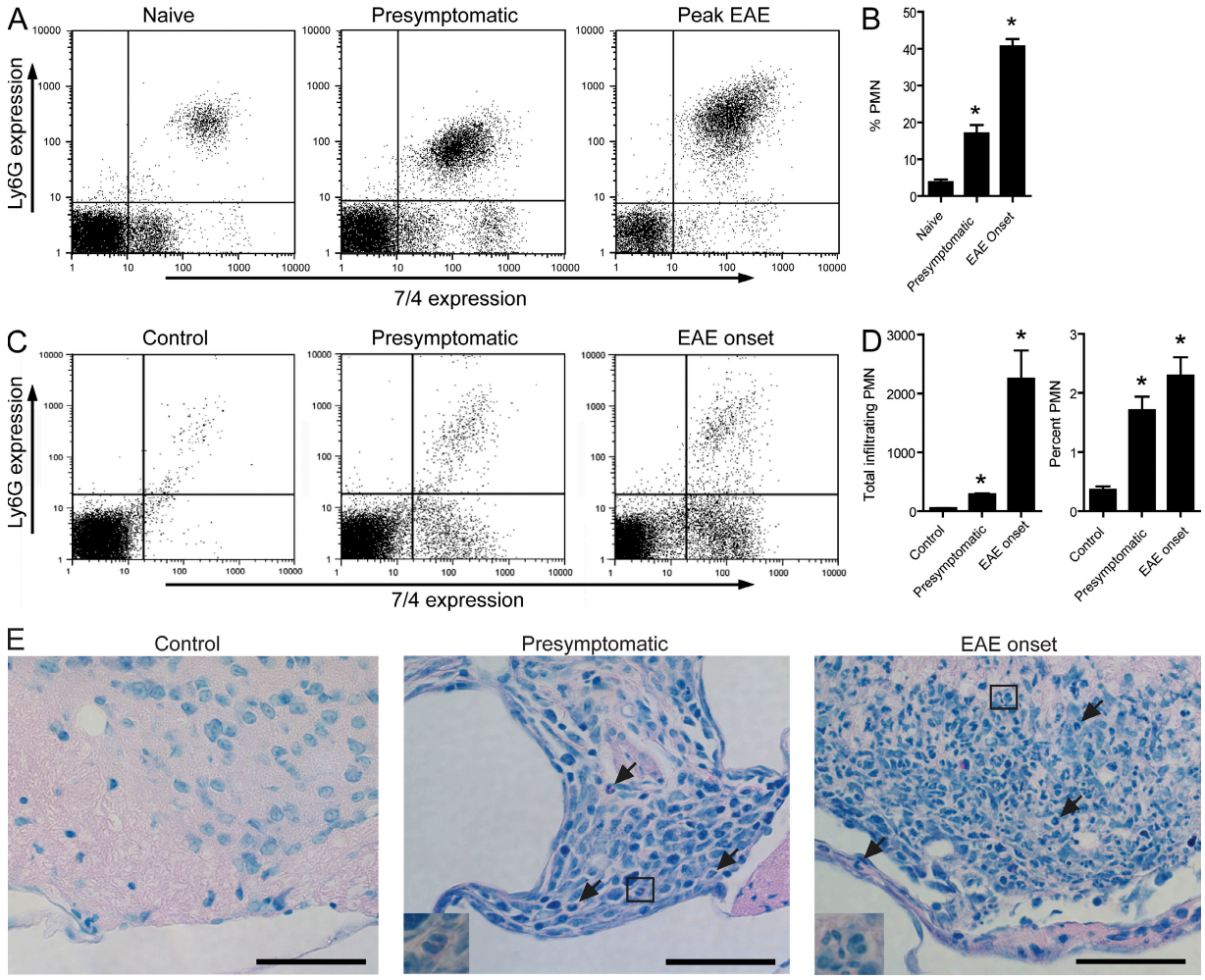

Figure 4. PMN accumulate in the blood and infiltrate the CNS during preclinical and active phases of EAE. (A and B) PBLs were analyzed by flow cytometry to determine the percentage of PMN (identified as Ly6G$^+$, 7/4$^+$, MHC class II$^-$ cells). (A) Representative FACS profiles. (B) Percentages of PMN among PBLs were averaged over four mice per group. *, $P < 0.001$ compared with naive mice. (C and D) Spinal cord–infiltrating cells were isolated and pooled from $PLP_{139-151}$–immunized SJL mice (n = 10–20) immediately before, or on the day of, clinical EAE onset. Cells from mice immunized with $NP_{260-183}$ served as controls. PMN were identified by FACS analysis as in A. (C) Representative FACS profiles gated on MHC class II$^-$ cells. (D) Total number of cells per cord and the percentage of CNS-infiltrating PMN. Data represent mean ± SD of four independent experiments. *, $P < 0.05$ compared with control. (E) Histological sections of spinal cords from $PLP_{139-151}$– and $NP_{260-283}$–immunized mice were Giemsa stained. PMN (arrows) are identified by their characteristic nuclear morphology (insets). The sections shown are representative of four mice per group. All experiments were repeated three or more times with consistent results. Bars, 50 µm.

T cell proliferation and Th1 polarization (28). PMN also secrete cytokines and chemokines that can directly modulate T cell differentiation (29, 30). Therefore we investigated the effects of PMN depletion on the priming of myelin-specific T cells in the periphery. CD4$^+$ T cells purified from the lymph nodes of PLP-immunized mice that had been injected either with RB6 or control antibodies mounted comparable lymphoproliferative and cytokine recall responses (Fig. 6, A and B). In contrast, RB6-treated mice failed to up-regulate IL-17, IFN-γ, or IL-6 in the CNS to the levels expressed in control mice at peak disease (Fig. 6 C). RB6 treatment also blocked CNS expression of PGRP, indicating that there was no detectable infiltration by PMN. Hence, reminiscent of our findings with the anti-CXCR2 antiserum, the therapeutic actions of RB6 are mediated during the effector stage, at a point after the generation of encephalitogenic CD4$^+$ T cells in secondary lymphoid organs, and correlate with inhibition of PMN trafficking to the CNS.

Resistance of CXCR2$^{-/-}$ mice is overcome by transfer of CXCR2$^{+/+}$ PMN

Although ELR$^+$ CXC chemokines are most widely characterized as attractants and activators of PMN, they can also mediate monocyte arrest (16). To determine whether CXCR2 expression on PMN is sufficient for EAE susceptibility, we injected CXCR2$^{-/-}$ mice with purified WT PMN over several days after immunization with PLP peptide. 100% of CXCR2$^{-/-}$ mice treated in this manner succumbed to clinical and histological EAE, although at a lower severity in comparison to

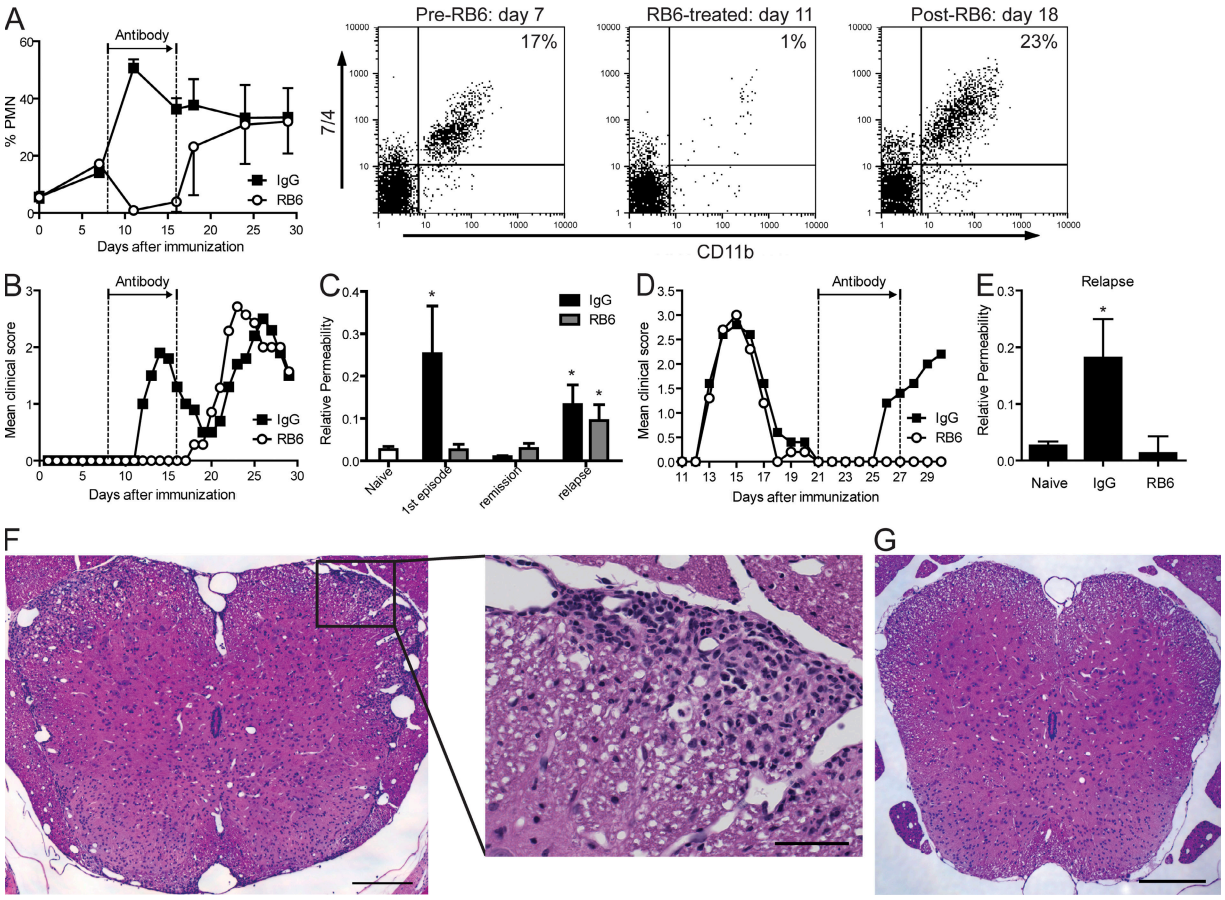

Figure 5. PMN depletion prevents BBB disruption and clinical and histopathological manifestations of EAE. SJL mice were injected with either RB6 or control IgG (0.5 mg per dose) every other day from days 8–16 (A–C, F, and G) or days 21–27 (D and E) after immunization with $PLP_{139-151}$ in CFA. (A) PBLs were collected at serial time points and analyzed by flow cytometry. PMN were identified as $CD11b^+$, $7/4^+$, MHC class II^- cells. The percentage of PMN was averaged over six mice per group. A representative FACS profile of each group is shown. Data represent mean ± SD. (B) Daily clinical scores were averaged over six mice in each group. (C) BBB integrity was assessed during the indicated stages of EAE in the control IgG–treated group by Evans blue dye extravasation. Data represent mean ± SD of six mice per group. *, $P < 0.05$ compared with naive mice. (D) The mean daily clinical score of each group ($n = 8$) is shown. (E) BBB integrity was assessed during the time of relapse in the control IgG–treated group. Data represent mean ± SD of six mice per group. *, $P < 0.05$ compared with naive mice. (F and G) Spinal cords were harvested and fixed on day 14 after immunization with $PLP_{139-151}$. Sections were Giemsa stained to visualize cell morphology. Images are representative of sections from four mice per group. All experiments were repeated three or more times with consistent results. Bars: (F, left; and G) 200 µm; (F, right) 50 µm.

PLP-immunized WT mice (Fig. 7 and Table I). $CXCR2^{-/-}$ mice injected with WT macrophages according to the same schedule remained resistant to EAE induction. PMN transfer induced BBB breakdown and CNS expression of IFN-γ and IL-6 in primed $CXCR2^{-/-}$ hosts, whereas macrophage transfer failed to do so (Fig. 8, A and B; and not depicted). Importantly, transfer of WT PMN resulted in CNS expression of PGRP and CXCR2, demonstrating that donor PMN homed to the target organ during the inflammatory process. Antigen-specific proliferation and cytokine secretion of lymph node $CD4^+$ T cells was comparable between PLP-primed WT and $CXCR2^{-/-}$ mice, as well as $CXCR2^{-/-}$ mice that received WT PMN transfers (Fig. 8, C and D).

DISCUSSION

The current study demonstrates that ELR^+ CXC chemokines and CXCR2-expressing PMN are required for the development of EAE. This is an unexpected finding in light of the current dogma regarding the immunopathogenesis of autoimmune demyelinating disease. Researchers studying EAE and other organ-specific autoimmune diseases have focused on the autoreactive T and/or B cells that guide pathological inflammation. Macrophages and, more recently, dendritic cells, have also received attention because of their role in presenting myelin antigens and in inflicting damage to the target organ (1, 31). Consequently, research involving chemokines in EAE has focused on the ML and ELR^- CXC chemokines that serve as the main chemoattractants for monocytes and lymphocytes (3, 4).

Although PMN are among the first leukocytes to infiltrate the CNS in some models of EAE (17), they are scarce in mature infiltrates. Hence, PMN have not generally been posited as key effector cells in popular theories on the pathogenesis of EAE or relapsing-remitting MS. Nonetheless, previous

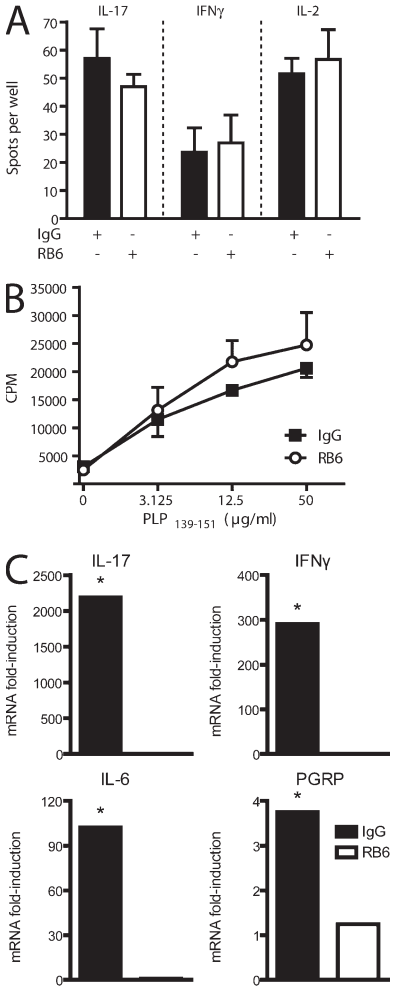

Figure 6. PLP-specific peripheral CD4⁺ responses are not altered by PMN depletion, but CNS up-regulation of inflammatory markers is blocked. (A and B) CD4⁺ T cells were isolated from draining lymph nodes of PLP-immunized SJL mice that had been treated with either control IgG (closed bars and squares) or RB6 (open bars and circles). The purified T cells were cultured with naive T cell–depleted splenocytes with or without 25 μg/ml PLP_{139151} for ELISPOT (A) and [^{3}H]thymidine uptake proliferation (B) assays. The ELISPOT data shown were generated by subtracting background spots (10 or fewer) that appeared in the absence of antigenic challenge. Data represent mean ± SD. (C) Spinal cords from PLP-immunized mice that had been treated with either control IgG or RB6 were analyzed by real-time RT-PCR. Data represent fold induction relative to naive spinal cords (n = 5 mice per group). *, $P < 0.05$ for IgG- compared with RB6-treated mice.

publications have demonstrated that ELR⁺ CXC chemokines, as well as other PMN-related factors such as leukotrienes and G-CSF, are up-regulated in the CNS during EAE and MS (6–8, 32, 33). CXCL8 was found to be elevated in the sera and peripheral blood mononuclear cells from MS patients in comparison to healthy volunteers (10). Furthermore, recombinant IFN-β, used in the clinical setting to suppress MS relapses, reduces CXCL8 expression in MS and inhibits both PMN infiltration of the CNS and BBB breakdown in animal models of neuroinflammation (10, 34). Conversely, administration of recombinant G-CSF was associated with acute relapses when given to MS patients undergoing bone marrow transplantation (35). Most strikingly, PMN depletion was recently reported to attenuate EAE induced either by active immunization or adoptive transfer (22). These observations are consistent with the results of our current study, which indicate that PMN-mobilizing and -activating factors play a critical role in facilitating autoimmune-mediated neuroinflammation and demyelination.

The mechanism of action of PMN in EAE remains to be elucidated. PMN produce chemokines and cytokines and participate in cell-to-cell interactions with dendritic cells that could modulate the differentiation and/or activation of lymphocytes and monocytes (28–30). However, our data indicate that PMN exert their functions during the effector rather than the induction phase of EAE because myelin-specific T cell expansion and Th1/Th17 differentiation were not impaired in either RB6-treated or CXCR2-deficient mice (Fig. 6, A and B; and Fig. 8, C and D). Furthermore, mice that were protected from EAE, either by anti-CXCR2 injection or PMN depletion, experienced exacerbations within days of treatment withdrawal (Fig. 3 A and Fig. 5 B). This indicates that encephalitogenic T cells had been generated in the periphery and were able to mediate disease as soon as functional PMN were available for collaboration. We and others (22) have found that PMN depletion suppresses EAE induced by the transfer of ordinarily encephalitogenic myelin-specific T cells (unpublished data). The ability of PMN to facilitate the trafficking and/or effector functions of memory T cells is not confined to autoimmune disease. Hence, CXCL1-dependent recruitment of PMN to cutaneous antigen challenge sites is required for the elicitation of contact hypersensitivity by previously primed, hapten-specific CD4⁺ and CD8⁺ T cells (36).

We postulate that PMN mediate or augment BBB breakdown during the period between the reactivation of myelin-specific T cells in the CNS and the massive influx of nonspecific leukocytes that heralds the onset of clinical EAE. In support of our hypothesis, PMN were recently shown to be important for increased vascular permeability and clinical disease in the K/BxN serum transfer model of arthritis (37). Furthermore, increased cerebrovascular permeability occurs in association with PMN infiltration of the CNS provoked by viral encephalitis, intracerebral injection of IL-1β or CXCL2, or by transgenic expression of CXCL1 in oligodendrocytes (38–42). In the case of the viral encephalitis and IL-1β injection models, depletion of PMN or neutralization of CXCL1 prevented compromise of the cerebrovasculature. Activated PMN can disrupt adherens junctions between endothelial cells via contact (β_2 integrin)-dependent pathways and via secretion of factors that trigger endothelial cell contraction (azurocidin and hydrogen peroxide), up-regulation of adhesion molecules (TNF and glutamate), and extracellular matrix degradation (elastase and other proteases) (43–47). In addition, the culture of activated PMN with brain endothelial

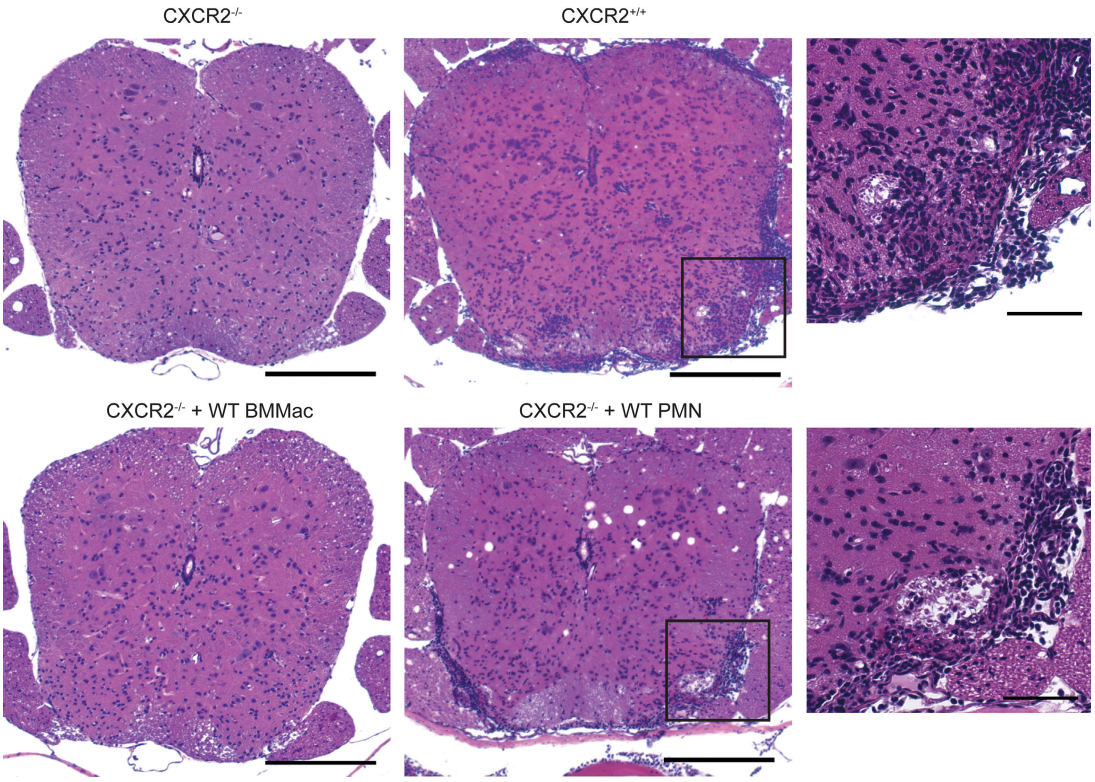

Figure 7. WT PMN promote neuroinflammation in myelin-immunized CXCR2$^{-/-}$ mice. BALB/c CXCR2$^{+/+}$ and CXCR2$^{-/-}$ mice were immunized with $PLP_{185-206}$ in CFA. CXCR2$^{-/-}$ mice were injected with 5×10^6 purified bone marrow PMN or BMMac daily between days 10 and 14 after immunization. Spinal cords were removed between days 13 and 15 after immunization, fixed, and hematoxylin and eosin stained. Representative sections of three mice per group are shown. Bars: (left and middle) 200 µm; (right) 50 µm.

cells triggers degradation of the adherens junction molecule β-catenin (48), and intracerebral injection of the PMN granule proteins neutrophil elastase and cathepsin G leads to BBB disruption (49).

Although we cannot conclude definitively that CXCR2$^+$ PMN act in such a fashion during EAE on the basis of the current study, both PMN depletion and CXCR2 blockade prevented BBB breakdown during initial clinical presentation and relapse (Fig. 3 and Fig. 5). Furthermore, WT PMN transfer was sufficient to promote vascular compromise in sensitized CXCR2-deficient mice (Fig. 8). Interestingly, in certain in vitro systems, PMN-induced changes in endothelial barrier function require cell-to-cell adherence but not transendothelial migration (50). This observation suggests that adhesion of PMN to the cerebrovascular wall alone might be sufficient to increase its permeability in vivo. If so, the seemingly paradoxical proposition that PMN are mechanistically involved in EAE despite composing a minor percentage of CNS-infiltrating cells would be reconciled.

Resistance of CXCR2$^{-/-}$ mice to EAE is reversed by the transfer of WT PMN (Table I, Fig. 7, and Fig. 8), indicating that ELR$^+$ CXC chemokines drive PMN-dependent events that are crucial for the development of clinical disease. The fact that CXCR2$^{-/-}$ mice supplemented with WT PMN experienced milder disease than WT littermates raises the possibility that expression of CXCR2 on cells other than PMN might also be important in this model of EAE. Nonetheless, our observation that PMN depletion and CXCR2 blockade have virtually identical effects on the clinical and histopathological features of EAE indicate that the ELR$^+$ CXC chemokine pathway induces the activation and/or migration of PMN in a nonredundant fashion. These results contrast with those of Abromson-Leeman et al., who reported that three out of four myelin-specific T cell lines successfully transferred EAE to naive CXCR2$^{-/-}$ mice (51). However, it is not clear that in vitro–derived T cell lines mimic the biological properties of endogenous pools of myelin-specific T cells activated in vivo.

Table I. WT PMN transfer restores EAE susceptibility in CXCR2$^{-/-}$ mice

	Incidence	Mean day of onset	Mean peak score
WT	100%	12.2	2.2
−/−	0%	–	0
WT PMN→−/−[a]	100%	13.5	1
WT BMMac→−/−[a]	0%	–	0

Data are representative of at least three independent experiments. WT, $n = 15$; −/−, $n = 12$; WT PMN→−/−, $n = 10$; WT BMMac→−/−, $n = 9$.
[a]5×10^6 cells transferred i.p. daily from day 10–14 after immunization.

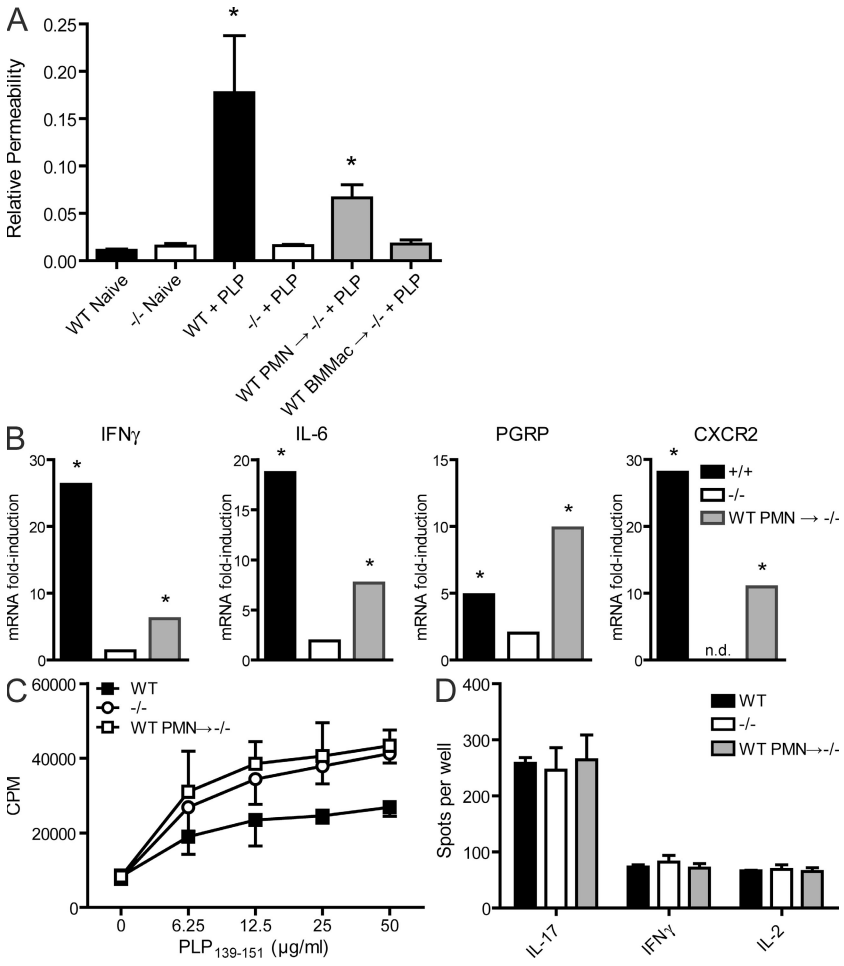

Figure 8. WT PMN induce BBB breakdown and CNS cytokine expression in myelin-immunized CXCR2$^{-/-}$ mice but do not affect peripheral CD4$^+$ T cell responses. BALB/c CXCR2$^{+/+}$ and CXCR2$^{-/-}$ mice were immunized with $PLP_{185-206}$ in CFA. CXCR2$^{-/-}$ mice were injected with 5×10^6 purified bone marrow PMN or BMMac daily between days 10 and 14 after immunization. (A) Cerebrovascular permeability was assessed by Evans blue dye extravasation on day 14 after immunization. Data represent mean ± SD. *, $P < 0.05$ compared with naive mice. (B) RNA was isolated from spinal cords between days 13 and 15 after immunization and analyzed by real-time RT-PCR. Data represent fold induction compared with naive spinal cords ($n = 4$ mice per group). *, $P < 0.03$ compared with CXCR2$^{-/-}$ mice. n.d., not detectable. (C and D) CD4$^+$ T cells were isolated from draining lymph nodes on day 14 after immunization. The purified T cells were cultured with naive T cell–depleted splenocytes plus or minus $PLP_{139-151}$. Lymphoproliferative and cytokine responses were measured by [^{3}H]thymidine uptake (C) and ELISPOT (D) assays, respectively. The ELISPOT data shown were generated by subtracting background spots (six or fewer) that appeared in the absence of antigenic challenge. Data represent mean ± SD.

Furthermore, recipients of the T cell lines were irradiated before adoptive transfer. If our theory is correct, Abromson-Leemans's protocol may have circumvented the requirement for PMN and ELR$^+$ CXC chemokines because irradiation, in and of itself, could trigger both immediate and long-term BBB disruption (52).

The results of our experiments dovetail nicely with reports from other laboratories that the IL-23–IL-17 axis plays a nonredundant role in the pathogenesis of EAE (53). Although Th17 cells have emerged as critical autoimmune effectors, the events linking IL-17 signaling to target organ inflammation and tissue damage are unknown. A major function of IL-17 is to induce production of ELR$^+$ CXC chemokines (54). CNS expression of ELR$^+$ CXC chemokines closely mirrors that of IL-17 during the relapsing-remitting course of EAE (Fig. 1), raising the possibility that IL-17 amplifies ELR$^+$ CXC chemokine production in EAE lesions as disease progresses. In fact, we have found that adoptive transfer of purified myelin-specific Th17, but not lineage-uncommitted, CD4$^+$ T cells triggers conspicuous CXCL1 and CXCL2 transcription in the CNS (Fig. 2 B). On the other hand, EAE induction by myelin-reactive Th1 cells is more closely associated with CNS up-regulation of ELR$^-$ than ELR$^+$ CXC chemokines (unpublished data).

Irrespective of the mechanism of action of PMN in EAE, the current study identifies ELR$^+$ CXC chemokines and the CXCR2/1 receptors as novel therapeutic targets in autoimmune diseases such as MS that might work synergistically with reagents that impede lymphocyte trafficking and/or function. This approach is particularly attractive, because

drugs that block PMN activation and/or adherence to the luminal surface of CNS vessels might be therapeutically effective without having to cross the BBB.

MATERIALS AND METHODS

Mice. SJL and BALB/c mice were purchased from the National Cancer Institute at 6–8 wk of age. BALB/c CXCR2$^{-/-}$, CXCR2$^{+/-}$, and CXCR2$^{+/+}$ mice littermates (originally purchased from Jackson ImmunoResearch Laboratories) were bred in our laboratory, as previously described (26). Mice were housed in a specific pathogen-free facility at the University of Rochester School of Medicine and Dentistry. All experiments were approved by the University of Rochester Committee on Animal Resources.

Antibodies and reagents. The following mAbs were purchased for flow cytometry: B220 (RA3-62), CD3 (145-2C11), CD4 (RM4-5), CD8 (53-6.7), CD11c (HL3), Ly6C (AL-21), Ly6G (1A8), MHC class II (7-16.17; BD Biosciences); 7/4 (Caltag and Serotec); and CD11b (M1/70), F4/80 (BM8), Gr-1 (RB6), and M-CSF R (AFS98; eBioscience). RB6 (Gr-1) mAbs were purified from hybridoma supernatants on protein G columns (GE Healthcare). Recombinant mouse M-CSF was purchased from PeproTech.

Induction and assessment of EAE. Mice were immunized subcutaneously over the flanks with 100 μg $PLP_{139-151}$ (SJL) or $PLP_{185-206}$ (BALB/c) in CFA containing 250 μg *Mycobacterium tuberculosis* H37RA (Difco). BALB/c mice were injected i.p. with 300 ng *Bordetella pertussis* toxin (List Biological Laboratories) on days 0 and 2 after immunization. Clinical assessment of EAE was performed according to the following criteria: 0, no disease; 1, limp tail; 2, hind-limb weakness; 3, partial hind-limb paralysis; 4, complete paralysis of one or more limbs; and 5, moribund state.

CXCR2 neutralization. Anti-CXCR2 antiserum was prepared by immunizing rabbits with a peptide (Met-Gly-Glu-Phe-Lys-Val-Asp-Lys-Phe-Asn-Ile-Glu-Asp-Phe-Phe-Ser-Gly) derived from the ligand binding site of CXCR2 (Biosynthesis) (13). To block CXCR2 in vivo, 0.5 ml of anti-CXCR2 antiserum was injected i.p. every third day. NRS was used as a control. Anti-CXCR2 antiserum failed to induce complement-mediated lysis of purified PMN in vitro or to deplete PMN (Ly6G$^+$, 7/4$^+$, MHC class II$^-$ cells) after in vivo administration of 0.5 ml i.p. every third day (unpublished data). The antiserum stained WT but not CXCR2$^{-/-}$ PMN (unpublished data).

Flow cytometric analysis. Cells were incubated with FcBlock (hybridoma 2.4G2; American Type Culture Collection) followed by biotinylated or fluorochrome-conjugated antibodies for 10 min on ice. For secondary staining, cells were washed and incubated with PerCP- or allophycocyanin-conjugated streptavidin for an additional 10 min. Data acquisition was performed on a flow cytometer (FACSCalibur; BD Biosciences) and analyzed with FlowJo software (Tree Star, Inc.).

Histology. Mice were perfused with 10% formalin, and vertebral columns were dissected and decalcified with Immunocal (Decal Chemical Corporation). Cords were fixed in 10% formalin, paraffin embedded, sectioned, and Giemsa stained. Images were captured on a microscope (Axioplan 2; Carl Zeiss, Inc.) with a SPOT camera and SPOT Advanced software (Diagnostic Instruments, Inc.).

CNS cell isolation. Mice were anesthetized with avertin and perfused with PBS by the intracardiac route. Spinal cords were minced and digested with 2 mg/ml of collagenase (CLS-4; Worthington Biochemical) and 1 mg/ml DNase I (DN25; Sigma-Aldrich) for 1 h at 37°C. Pooled spinal cord cells were layered over a discontinuous Percoll gradient, centrifuged for 25 min at 2,500 rpm, and collected from the 30/70% interface.

In vitro T cell assays. CD4$^+$ T cells were purified from pooled lymph nodes and spleens using CD4$^+$ T cell enrichment columns (Cedarlane Laboratories). Spleens were depleted of T cells by complement-mediated lysis with J1J (anti-Thy1.2) hybridoma supernatants and guinea pig complement (Rockland Immunochemicals). Purified CD4$^+$ T cells were cultured with T cell–depleted splenocytes at a ratio of 1:4 (5×10^5 cells/well in 0.2 ml of tissue culture media) and stimulated in vitro with 25 μg/ml of either $PLP_{139-151}$ (SJL) or $PLP_{185-206}$ (BALB/c) media, or 0.5 μg/ml anti-CD3. For proliferation experiments, cells were cultured in flat-bottom 96-well plates for 96 h. 1 μCi/well [^{3}H]thymidine (GE Healthcare) was added for the last 16 h of culture. Incorporated radioactivity was measured using a scintillation counter (Betaplate; PerkinElmer). ELISPOT assays were performed in 96-well filtration plates (Millipore) with noncompeting antibody pairs. Cells were cultured (100 μl/well at 37°C) with or without 50 μg/ml of antigen for 24 h before application of biotinylated secondary antibodies and streptavidin-alkaline phosphatase. Plates were developed with Vector Blue (Vector Laboratories), and spots were counted using an analyzer (CTL ImmunoSpot) with ImmunoSpot software (version 2.08; both from Cellular Technology). All assays were performed in triplicate.

BBB permeability. Mice were injected i.v. with 2% Evans blue dye (0.01 ml/g; Sigma-Aldrich) and perfused with PBS by the intracardiac route 2 h later. Spinal cord and kidney samples were homogenized in formamide (20 ml/g of tissue wet weight; Sigma-Aldrich), and dye was extracted overnight. After centrifugation at 21,000 *g* for 30 min, supernatants were removed and absorbance was measured at 620 and 740 nm. Background absorbance (calculated as $-\log OD_{620} = (0.964)(-\log OD_{740}) - 0.0357$) was subtracted to obtain the data shown in the figures, as previously described (55). Relative permeability represents the ratio of Evans blue extravasation (micrograms of dye per gram of tissue) from spinal cord homogenates to kidney homogenates.

Real-time RT-PCR. RNA was isolated with TRIzol (Invitrogen) according to the manufacturer's protocol. cDNA was synthesized with a reverse transcription kit (QuantiTect; QIAGEN). PCR was performed using a single-color real-time PCR detection system (MyiQ; Bio-Rad Laboratories). Primers and probes were designed with Beacon Designer (Premier Biosoft International). Samples were amplified over 40 cycles according to the following protocol: 15 s at 95°C, 1 min at 60°C. Target gene expression was normalized to GAPDH. The relative expression of mRNA in tissues from immunized mice versus naive mice was determined using the REST-XL software tool (version 2) (56), and data are represented as fold induction compared with naive controls. General trends and statistical significance were similar when β-actin was used as the housekeeping gene (unpublished data).

Cell transfer experiments. PMN (>97% purity) were isolated from bone marrow using anti–Ly6G-biotin and antibiotin microbeads (Miltenyi Biotec). Enriched bone marrow macrophages (BMMac; 82–87% purity) were enriched from whole bone marrow cells by culture with 10 ng/ml M-CSF. After 5 d, adherent cells were harvested and isolated over a 62% Percoll gradient by centrifugation for 30 min at 1,500 *g*. Ly6G$^+$ cells were removed with anti–Ly6G-biotin/antibiotin beads. Cytospins and flow cytometry were used to confirm cellular purity (Fig. S2, available at http://www.jem.org/cgi/content/full/jem.20072404/DC1). Recipient mice were injected with 5×10^6 PMN or BMMac i.p.

Statistical analysis. Real-time RT-PCR data were analyzed by the pairwise fixed reallocation randomization test with REST-XL software (version 2). All other data were analyzed by the Mann-Whitney test with Prism 5 software (GraphPad Software).

Online supplemental material. Fig. S1 shows the PMN depletion efficiency and specificity of the RB6 mAb on PBL subsets. Fig. S2 shows the purity of PMN and BMMac used for transfer into CXCR2$^{-/-}$ mice. Online supplemental material is available at http://www.jem.org/cgi/content/full/jem.20072404/DC1.

This work was supported by grants from the National Multiple Sclerosis Society (RG 3866-A-3) and the National Institutes of Health (NS047687-01A1 and NS041249). B.M. Segal was a Harry Weaver Neuroscience Scholar of the National Multiple Sclerosis Society.

The authors have no conflicting financial interests.

Submitted: 12 November 2007
Accepted: 15 February 2008

REFERENCES

1. Fischer, H.G., and G. Reichmann. 2001. Brain dendritic cells and macrophages/microglia in central nervous system inflammation. *J. Immunol.* 166:2717–2726.
2. Traugott, U., C.S. Raine, and D.E. McFarlin. 1985. Acute experimental allergic encephalomyelitis in the mouse: immunopathology of the developing lesion. *Cell. Immunol.* 91:240–254.
3. Karpus, W.J., and R.M. Ransohoff. 1998. Chemokine regulation of experimental autoimmune encephalomyelitis: temporal and spatial expression patterns govern disease pathogenesis. *J. Immunol.* 161:2667–2671.
4. Rebenko-Moll, N.M., L. Liu, A. Cardona, and R.M. Ransohoff. 2006. Chemokines, mononuclear cells and the nervous system: heaven (or hell) is in the details. *Curr. Opin. Immunol.* 18:683–689.
5. Fischer, F.R., L. Santambrogio, Y. Luo, M.A. Berman, W.W. Hancock, and M.E. Dorf. 2000. Modulation of experimental autoimmune encephalomyelitis: effect of altered peptide ligand on chemokine and chemokine receptor expression. *J. Neuroimmunol.* 110:195–208.
6. Glabinski, A.R., M. Tani, R.M. Strieter, V.K. Tuohy, and R.M. Ransohoff. 1997. Synchronous synthesis of alpha- and beta-chemokines by cells of diverse lineage in the central nervous system of mice with relapses of chronic experimental autoimmune encephalomyelitis. *Am. J. Pathol.* 150:617–630.
7. Glabinski, A.R., V.K. Tuohy, and R.M. Ransohoff. 1998. Expression of chemokines RANTES, MIP-1alpha and GRO-alpha correlates with inflammation in acute experimental autoimmune encephalomyelitis. *Neuroimmunomodulation.* 5:166–171.
8. Godiska, R., D. Chantry, G.N. Dietsch, and P.W. Gray. 1995. Chemokine expression in murine experimental allergic encephalomyelitis. *J. Neuroimmunol.* 58:167–176.
9. Ishizu, T., M. Osoegawa, F.J. Mei, H. Kikuchi, M. Tanaka, Y. Takakura, M. Minohara, H. Murai, F. Mihara, T. Taniwaki, and J. Kira. 2005. Intrathecal activation of the IL-17/IL-8 axis in opticospinal multiple sclerosis. *Brain.* 128:988–1002.
10. Lund, B.T., N. Ashikian, H.Q. Ta, Y. Chakryan, K. Manoukian, S. Groshen, W. Gilmore, G.S. Cheema, W. Stohl, M.E. Burnett, et al. 2004. Increased CXCL8 (IL-8) expression in Multiple Sclerosis. *J. Neuroimmunol.* 155:161–171.
11. Del Rio, L., S. Bennouna, J. Salinas, and E.Y. Denkers. 2001. CXCR2 deficiency confers impaired neutrophil recruitment and increased susceptibility during *Toxoplasma gondii* infection. *J. Immunol.* 167:6503–6509.
12. Kielian, T., B. Barry, and W.F. Hickey. 2001. CXC chemokine receptor-2 ligands are required for neutrophil-mediated host defense in experimental brain abscesses. *J. Immunol.* 166:4634–4643.
13. Mehrad, B., R.M. Strieter, T.A. Moore, W.C. Tsai, S.A. Lira, and T.J. Standiford. 1999. CXC chemokine receptor-2 ligands are necessary components of neutrophil-mediated host defense in invasive pulmonary aspergillosis. *J. Immunol.* 163:6086–6094.
14. Podolin, P.L., B.J. Bolognese, J.J. Foley, D.B. Schmidt, P.T. Buckley, K.L. Widdowson, Q. Jin, J.R. White, J.M. Lee, R.B. Goodman, et al. 2002. A potent and selective nonpeptide antagonist of CXCR2 inhibits acute and chronic models of arthritis in the rabbit. *J. Immunol.* 169:6435–6444.
15. Takaoka, A., Y. Tanaka, T. Tsuji, T. Jinushi, A. Hoshino, Y. Asakura, Y. Mita, K. Watanabe, S. Nakaike, Y. Togashi, et al. 2001. A critical role for mouse CXC chemokine(s) in pulmonary neutrophilia during Th type 1-dependent airway inflammation. *J. Immunol.* 167:2349–2353.
16. Boisvert, W.A., D.M. Rose, K.A. Johnson, M.E. Fuentes, S.A. Lira, L.K. Curtiss, and R.A. Terkeltaub. 2006. Up-regulated expression of the CXCR2 ligand KC/GRO-alpha in atherosclerotic lesions plays a central role in macrophage accumulation and lesion progression. *Am. J. Pathol.* 168:1385–1395.
17. Brown, A., D.E. McFarlin, and C.S. Raine. 1982. Chronologic neuropathology of relapsing experimental allergic encephalomyelitis in the mouse. *Lab. Invest.* 46:171–185.
18. Huang, D.R., J. Wang, P. Kivisakk, B.J. Rollins, and R.M. Ransohoff. 2001. Absence of monocyte chemoattractant protein 1 in mice leads to decreased local macrophage recruitment and antigen-specific T helper cell type 1 immune response in experimental autoimmune encephalomyelitis. *J. Exp. Med.* 193:713–726.
19. Komiyama, Y., S. Nakae, T. Matsuki, A. Nambu, H. Ishigame, S. Kakuta, K. Sudo, and Y. Iwakura. 2006. IL-17 plays an important role in the development of experimental autoimmune encephalomyelitis. *J. Immunol.* 177:566–573.
20. Matusevicius, D., P. Kivisakk, B. He, N. Kostulas, V. Ozenci, S. Fredrikson, and H. Link. 1999. Interleukin-17 mRNA expression in blood and CSF mononuclear cells is augmented in multiple sclerosis. *Mult. Scler.* 5:101–104.
21. Park, H., Z. Li, X.O. Yang, S.H. Chang, R. Nurieva, Y.H. Wang, Y. Wang, L. Hood, Z. Zhu, Q. Tian, and C. Dong. 2005. A distinct lineage of CD4 T cells regulates tissue inflammation by producing interleukin 17. *Nat. Immunol.* 6:1133–1141.
22. McColl, S.R., M.A. Staykova, A. Wozniak, S. Fordham, J. Bruce, and D.O. Willenborg. 1998. Treatment with anti-granulocyte antibodies inhibits the effector phase of experimental autoimmune encephalomyelitis. *J. Immunol.* 161:6421–6426.
23. Lucchinetti, C.F., R.N. Mandler, D. McGavern, W. Bruck, G. Gleich, R.M. Ransohoff, C. Trebst, B. Weinshenker, D. Wingerchuk, J.E. Parisi, and H. Lassmann. 2002. A role for humoral mechanisms in the pathogenesis of Devic's neuromyelitis optica. *Brain.* 125:1450–1461.
24. Tran, E.H., E.N. Prince, and T. Owens. 2000. IFN-gamma shapes immune invasion of the central nervous system via regulation of chemokines. *J. Immunol.* 164:2759–2768.
25. Liu, C., E. Gelius, G. Liu, H. Steiner, and R. Dziarski. 2000. Mammalian peptidoglycan recognition protein binds peptidoglycan with high affinity, is expressed in neutrophils, and inhibits bacterial growth. *J. Biol. Chem.* 275:24490–24499.
26. Cacalano, G., J. Lee, K. Kikly, A.M. Ryan, S. Pitts-Meek, B. Hultgren, W.I. Wood, and M.W. Moore. 1994. Neutrophil and B cell expansion in mice that lack the murine IL-8 receptor homolog. *Science.* 265:682–684.
27. Conlan, J.W., and R.J. North. 1994. Neutrophils are essential for early anti-Listeria defense in the liver, but not in the spleen or peritoneal cavity, as revealed by a granulocyte-depleting monoclonal antibody. *J. Exp. Med.* 179:259–268.
28. van Gisbergen, K.P., M. Sanchez-Hernandez, T.B. Geijtenbeek, and Y. van Kooyk. 2005. Neutrophils mediate immune modulation of dendritic cells through glycosylation-dependent interactions between Mac-1 and DC-SIGN. *J. Exp. Med.* 201:1281–1292.
29. Bennouna, S., S.K. Bliss, T.J. Curiel, and E.Y. Denkers. 2003. Cross-talk in the innate immune system: neutrophils instruct recruitment and activation of dendritic cells during microbial infection. *J. Immunol.* 171:6052–6058.
30. Scapini, P., J.A. Lapinet-Vera, S. Gasperini, F. Calzetti, F. Bazzoni, and M.A. Cassatella. 2000. The neutrophil as a cellular source of chemokines. *Immunol. Rev.* 177:195–203.
31. Tran, E.H., K. Hoekstra, N. van Rooijen, C.D. Dijkstra, and T. Owens. 1998. Immune invasion of the central nervous system parenchyma and experimental allergic encephalomyelitis, but not leukocyte extravasation from blood, are prevented in macrophage-depleted mice. *J. Immunol.* 161:3767–3775.
32. Lock, C., G. Hermans, R. Pedotti, A. Brendolan, E. Schadt, H. Garren, A. Langer-Gould, S. Strober, B. Cannella, J. Allard, et al. 2002. Gene-microarray analysis of multiple sclerosis lesions yields new targets validated in autoimmune encephalomyelitis. *Nat. Med.* 8:500–508.
33. Whitney, L.W., S.K. Ludwin, H.F. McFarland, and W.E. Biddison. 2001. Microarray analysis of gene expression in multiple sclerosis and EAE identifies 5-lipoxygenase as a component of inflammatory lesions. *J. Neuroimmunol.* 121:40–48.

34. Veldhuis, W.B., S. Floris, P.H. van der Meide, I.M. Vos, H.E. de Vries, C.D. Dijkstra, P.R. Bar, and K. Nicolay. 2003. Interferon-beta prevents cytokine-induced neutrophil infiltration and attenuates blood-brain barrier disruption. *J. Cereb. Blood Flow Metab.* 23:1060–1069.
35. Openshaw, H., O. Stuve, J.P. Antel, R. Nash, B.T. Lund, L.P. Weiner, A. Kashyap, P. McSweeney, and S. Forman. 2000. Multiple sclerosis flares associated with recombinant granulocyte colony-stimulating factor. *Neurology.* 54:2147–2150.
36. Dilulio, N.A., T. Engeman, D. Armstrong, C. Tannenbaum, T.A. Hamilton, and R.L. Fairchild. 1999. Groalpha-mediated recruitment of neutrophils is required for elicitation of contact hypersensitivity. *Eur. J. Immunol.* 29:3485–3495.
37. Binstadt, B.A., P.R. Patel, H. Alencar, P.A. Nigrovic, D.M. Lee, U. Mahmood, R. Weissleder, D. Mathis, and C. Benoist. 2006. Particularities of the vasculature can promote the organ specificity of autoimmune attack. *Nat. Immunol.* 7:284–292.
38. Anthony, D., R. Dempster, S. Fearn, J. Clements, G. Wells, V.H. Perry, and K. Walker. 1998. CXC chemokines generate age-related increases in neutrophil-mediated brain inflammation and blood-brain barrier breakdown. *Curr. Biol.* 8:923–926.
39. Anthony, D.C., S.J. Bolton, S. Fearn, and V.H. Perry. 1997. Age-related effects of interleukin-1 beta on polymorphonuclear neutrophil-dependent increases in blood-brain barrier permeability in rats. *Brain.* 120:435–444.
40. Tani, M., M.E. Fuentes, J.W. Peterson, B.D. Trapp, S.K. Durham, J.K. Loy, R. Bravo, R.M. Ransohoff, and S.A. Lira. 1996. Neutrophil infiltration, glial reaction, and neurological disease in transgenic mice expressing the chemokine N51/KC in oligodendrocytes. *J. Clin. Invest.* 98:529–539.
41. Bell, M.D., D.D. Taub, and V.H. Perry. 1996. Overriding the brain's intrinsic resistance to leukocyte recruitment with intraparenchymal injections of recombinant chemokines. *Neuroscience.* 74:283–292.
42. Zhou, J., S.A. Stohlman, D.R. Hinton, and N.W. Marten. 2003. Neutrophils promote mononuclear cell infiltration during viral-induced encephalitis. *J. Immunol.* 170:3331–3336.
43. Collard, C.D., K.A. Park, M.C. Montalto, S. Alapati, J.A. Buras, G.L. Stahl, and S.P. Colgan. 2002. Neutrophil-derived glutamate regulates vascular endothelial barrier function. *J. Biol. Chem.* 277:14801–14811.
44. Del Maschio, A., A. Zanetti, M. Corada, Y. Rival, L. Ruco, M.G. Lampugnani, and E. Dejana. 1996. Polymorphonuclear leukocyte adhesion triggers the disorganization of endothelial cell-to-cell adherens junctions. *J. Cell Biol.* 135:497–510.
45. Gautam, N., H. Herwald, P. Hedqvist, and L. Lindbom. 2000. Signaling via β_2 integrins triggers neutrophil-dependent alteration in endothelial barrier function. *J. Exp. Med.* 191:1829–1839.
46. Gautam, N., A.M. Olofsson, H. Herwald, L.F. Iversen, E. Lundgren-Akerlund, P. Hedqvist, K.E. Arfors, H. Flodgaard, and L. Lindbom. 2001. Heparin-binding protein (HBP/CAP37): a missing link in neutrophil-evoked alteration of vascular permeability. *Nat. Med.* 7:1123–1127.
47. Ionescu, C.V., G. Cepinskas, J. Savickiene, M. Sandig, and P.R. Kvietys. 2003. Neutrophils induce sequential focal changes in endothelial adherens junction components: role of elastase. *Microcirculation.* 10:205–220.
48. Schuller, A.M., J. Windolf, R. Blaheta, J. Cinatl, J. Kreuter, G. Wimmer-Greinecker, A. Moritz, and M. Scholz. 2005. Degradation of microvascular brain endothelial cell beta-catenin after co-culture with activated neutrophils from patients undergoing cardiac surgery with prolonged cardiopulmonary bypass. *Biochem. Biophys. Res. Commun.* 329:616–623.
49. Armao, D., M. Kornfeld, E.Y. Estrada, M. Grossetete, and G.A. Rosenberg. 1997. Neutral proteases and disruption of the blood-brain barrier in rat. *Brain Res.* 767:259–264.
50. Gautam, N., P. Hedqvist, and L. Lindbom. 1998. Kinetics of leukocyte-induced changes in endothelial barrier function. *Br. J. Pharmacol.* 125:1109–1114.
51. Abromson-Leeman, S., R. Bronson, Y. Luo, M. Berman, R. Leeman, J. Leeman, and M. Dorf. 2004. T-cell properties determine disease site, clinical presentation, and cellular pathology of experimental autoimmune encephalomyelitis. *Am. J. Pathol.* 165:1519–1533.
52. Nordal, R.A., and C.S. Wong. 2005. Molecular targets in radiation-induced blood-brain barrier disruption. *Int. J. Radiat. Oncol. Biol. Phys.* 62:279–287.
53. Cua, D.J., J. Sherlock, Y. Chen, C.A. Murphy, B. Joyce, B. Seymour, L. Lucian, W. To, S. Kwan, T. Churakova, et al. 2003. Interleukin-23 rather than interleukin-12 is the critical cytokine for autoimmune inflammation of the brain. *Nature.* 421:744–748.
54. Kolls, J.K., and A. Linden. 2004. Interleukin-17 family members and inflammation. *Immunity.* 21:467–476.
55. Warnick, R.E., J.R. Fike, P.H. Chan, D.K. Anderson, G.Y. Ross, and P.H. Gutin. 1995. Measurement of vascular permeability in spinal cord using Evans Blue spectrophotometry and correction for turbidity. *J. Neurosci. Methods.* 58:167–171.
56. Pfaffl, M.W., G.W. Horgan, and L. Dempfle. 2002. Relative expression software tool (REST) for group-wise comparison and statistical analysis of relative expression results in real-time PCR. *Nucleic Acids Res.* 30:e36.